DEFENSE TECHNICAL INFORMATION CENTER

Information for the Defense Community

DTIC® has determined on 01/05/2011 that this Technical Document has the Distribution Statement checked below. The current distribution for this document can be found in the DTIC® Technical Report Database.

☒ **DISTRIBUTION STATEMENT A.** Approved for public release; distribution is unlimited.

☐ **© COPYRIGHTED.** U.S. Government or Federal Rights License. All other rights and uses except those permitted by copyright law are reserved by the copyright owner.

☐ **DISTRIBUTION STATEMENT B.** Distribution authorized to U.S. Government agencies only (fill in reason) (date of determination). Other requests for this document shall be referred to (insert controlling DoD office).

☐ **DISTRIBUTION STATEMENT C.** Distribution authorized to U.S. Government Agencies and their contractors (fill in reason) (date determination). Other requests for this document shall be referred to (insert controlling DoD office).

☐ **DISTRIBUTION STATEMENT D.** Distribution authorized to the Department of Defense and U.S. DoD contractors only (fill in reason) (date of determination). Other requests shall be referred to (insert controlling DoD office).

☐ **DISTRIBUTION STATEMENT E.** Distribution authorized to DoD Components only (fill in reason) (date of determination). Other requests shall be referred to (insert controlling DoD office).

☐ **DISTRIBUTION STATEMENT F.** Further dissemination only as directed by (insert controlling DoD office) (date of determination) or higher DoD authority.

Distribution Statement F is also used when a document does not contain a distribution statement and no distribution statement can be determined.

☐ **DISTRIBUTION STATEMENT X.** Distribution authorized to U.S. Government Agencies and private individuals or enterprises eligible to obtain export-controlled technical data in accordance with DoDD 5230.25; (date of determination). DoD Controlling Office is (insert controlling DoD office).

751173

An Experimentally Validated 3-D Inertial Tracking Package for Application in Biodynamic Research

E. Becker and G. Willems
Naval Aerospace Medical Research Laboratory Detachment

Abstract

A six-accelerometer inertial tracking package currently in intensive use in measuring living human and human surrogate response to impact acceleration is presented and discussed. The discussion includes an enumeration of the various requirements imposed upon the package as well os its design and fabrication.

The on-site calibration facility is described, including a discussion of the procedures for routine calibration of the pockoges. Accounts of the data acquisition link from the packoges through the sled borne amplifiers to the hybrid computer are also included.

Particular attention is devoted to the theoretical aspects of this system. A statement of errors is developed and compared to the various precision parameters of this system and to a general estimation of the dynamic response envelope demonstrating the overall feasibility of this approach.

THE NAVAL AEROSPACE MEDICAL RESEARCH LABORATORY DETACHMENT, New Orleans, is currently engaged in a series of experiments to determine human dynamic response to impact acceleration. Using a sled driven by a pneumotic occelerator, human volunteers and such human surrogates as large primates and anthropomorphic dummies ore subjected to short durotion accelerations approximating crash situations and their responses are monitored by a wide ronge of measurement systems.

These measurement systems fall into one of three main categories: Physiological, Optical, and Inertial. The physiological systems include electroencephalography, electrocardiography, ond electrooculography. The optical systems include high speed cinematography (1) and television. The inertial systems include sled mounted accelerometers, subject mounted

biaxial rate gyroscopes, and the subject mounted subminiature inertial tracking packages that are the topic of this report.

Systems in the first of these categories provide time histories of the volunteer subject's electrophysiological status while systems in the next two categories provide time histories of the impact itself as well as the kinematic response of instrumented segments of the subject's anatomy. This information is required for the design and validation of anthropomorphic dummies and of vehicular impact protection systems, and in the measurement of a crash victim's ability to perform escape or fire control maneuvers immediately after the impact.

THE SYSTEM

Each subminiature inertial tracking package consists in brief of six accelerometers mounted on an aluminum body that is in turn fixed to the subject anatomy. Three of these accelerometers are grouped near a single point and provide essentially, the translational acceleration of that point. Two more accelerometers are located about a second point and, used in conjunction with the first three accelerometers provide two of the three components of angular acceleration. A single accelerometer at still another point then yields the third component of the angular acceleration. Of course, many refinements of this discussion are necessary in order to work up and implement this system, but the most concise description is that of the six-accelerometer system in a three-two-one configuration as shown in Figure 1.

These tracking packages are designed to meet a wide range of requirements. These can be grouped in three general categories: The first of these being the requirements imposed by the nature of human kinematic response to impact such as dynamic range, duration, bandpass, and dimensionality; the second category consists of limitations on the size, mass, rotational inertias, and mountings of the devices so that the wearing of the systems produces no significant perturbations upon the kinematic response. The final category is composed of those requirements consistent with the efficient and economical operation and maintenance of the devices.

The nature of human kinematic response to impact acceleration has been the subject of a number of earlier studies: The joint Army-Navy-Wayne State University investigation presented by Ewing, et al (2)(3)(4) at the 12th and 13th Stapp Car Crash Conferences and reported in NAMRL Monograph 21; work done at

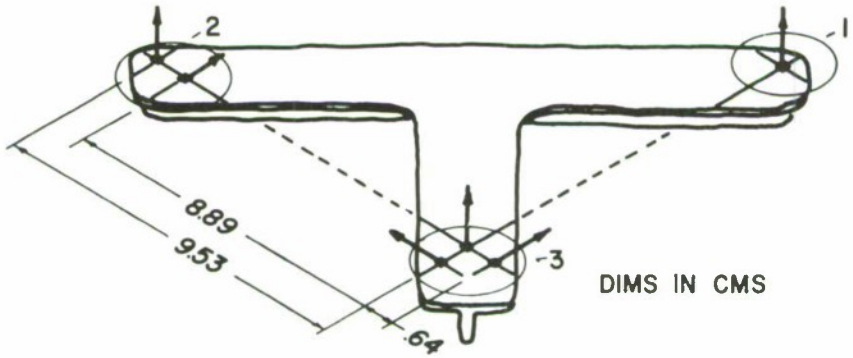

Fig. 1 - The six-accelerometer system, 3-2-1 configuration

Holloman Air Force Base and reported by Bendixen (5) and Clarke (6); and work done ot W. Stote University reported by Mertz and Patrick (7).

In eoch of these studies the motions of head (and in the work reported by Ewing et al, the first thoracic vertebral body as well) were measured in terms of the rigid body motion of some coordinate system fixed in the anatomy. Since the impact vectors were confined to the midsaggital plane, the assumption of symmetry reduces these motions to three degrees of freedom per anatomical body; two degrees of translation within the midsaggital plane and a single rotation about an axis perpendicular to this plane. Although this earlier work is concerned with impact vectors situated in the subject midsaggitol plane, on examination of the results suggests the following generalizations concerning human kinematic response to impact.

1. The domain of response begins ot the initiation of impoct and lasts from 200 to 350 milliseconds.

2. The response hos significont frequency components from d.c. to 30 to 50 Hz.

The approximation of rigid body motion is retained in this current work, but a global range of impact vectors is anticipated invalidating the assumption of planar motion. Therefore, six kinematic parameters must be monitored for each rigid body.

The problems encountered in the design and implementation of the anatomical mountings for these packages are too numerous and complex to be addressed here. But the limitations imposed on pockage size, mass, and rotational inertia that develop from these same anatomical considerations are the most important factors bearing on the package design.

At the outset of the design phase, a choice was to be made concerning the inertial transducer types to be incorporated in the packages. A study of commercially available instrumentation had narrowed the design options to packages consisting solely of subminiature piezoresistive accelerometers, or packages consisting of a number of rate gyroscopes as well as these piezoresistive accelerometers.

The masses of the accelerometers are virtually negligible, but the masses of rate gyroscopes range from about 80 gms for the Northrop Corp. Biaxial Rate Transducer ta 100 gms for the single axis Fairchild and U.S. Time Devices. Accommodations for the flange mountings on these transducers could be expected to add another 15 to 25 gms. The result is that if nominal values for head mass and head rotational inertia about the Y axis, as in nodding, are taken as 4000 gms and 2.30×10^5 gm-cm^2 respectively, (as in ref. (8)), that while penalties af anly 2% ta 3% additianal mass are incurred per transducer the corresponding increase in rotational inertia is about 10% when the anatomical mounting is at the mouth. These additional increases in rotational inertia were deemed unacceptable, expecially at the upper end of the range of impact levels included in the experimental design.

The requirements consistent with the operation and maintenance of these devices call for the minimization of associated sled borne equipment such as amplifiers and the like and the minimization of the channels of information transmitted via hard-wire whip cable to the data collection systems. These requirements also call for modularization of the separate transducers used to instrument an anatomical body. The concept of subminiature inertial tracking packages is in fact a marriage of convenience in which a number of elements are joined to produce a single albeit complex entity with associated calibration procedures and parameters.

The initial expense necessitated by this modular concept is greater; entire modules must be maintained as backup instrumentation rather than a few extra transducers. This expense is offset by the ease with which these modules can be deployed and interchanged and by the savings in bookkeeping necessary to document the impact experiments. Moreover, the minimal physical dimensions of the piezoresistive accelerometers has so complicated the task of locating them, that anything less than permanent mounting becomes uneconomical.

The subminiature inertial tracking packages consist of six piezoresistive accelerometers fixed to a ribbed, aluminum 'tee' in a rigidly controlled geometrical configuration. This 'tee'

then mates mechanically in a precise and reproducible fashion with the various onatomical mountings.

The rib, which is necessary to raise the natural frequency of flexural vibration above the bandwidth of the kinematic response, precludes the economical machining of these 'tees' from aluminum stock in quantity; instead these 'tees' ore sand-cast. Then only the surface opposite the ribs need be machined to mate with the anatomical mountings and scribed for the accelerometer placement. The 'tee' is then sent to Entran Devices where the accelerometers. are custom mounted on the scribed surface.

These accelerometers are availoble off the shelf in o variety of acceleration ranges and are damped to minimize spurious resonances providing a bandwidth from d.c. to 500 Hz or more.

Since these transducers are designed for a wide range of applications in which the standards of accuracy and linearity are not as stringent as those necessary for the tracking packages, a preselection process identifies the devices best suited for this work. Batches of accelerometers are sent to NAMRL for testing on the in-house calibration facility. Those meeting lab standards are earmarked for inclusion in the tracking packages and the entire batch is returned to the monufocturer.

The earmarked transducers are then epoxied to the machined 'tee' surface to within two thausandths of an inch of the scribed position. The temperature compensation modules are attached at convenient sites along the rib. Finally, the leads from all six accelerameters are dressed out three feet from the assembly ond terminated on a single connector that mates with the sled borne amplifiers.

Various stages of this work-up are shown in Figures 2 and 3; the raugh castings, the machined surface with and without transducers, and the final assembly complete with photographic targets. Figure 4 shows an instrumented human volunteer.

SYSTEM CALIBRATION

These inertial tracking packoges are calibrated at regular intervals on the same facility used to preselect the accelerometers. This calibration facility, diagrammed in Figure 5, consists of an Inland Controls 800 series® rate table interfaced with the EAI Pacer® 600 hybrid computer used in the data acquisition system (DAS).

This rate table has a twenty-four inch diameter table top and develops angular velocities of up to ten thousand degrees

Fig. 2 - Tee-rough castings and the machined surface

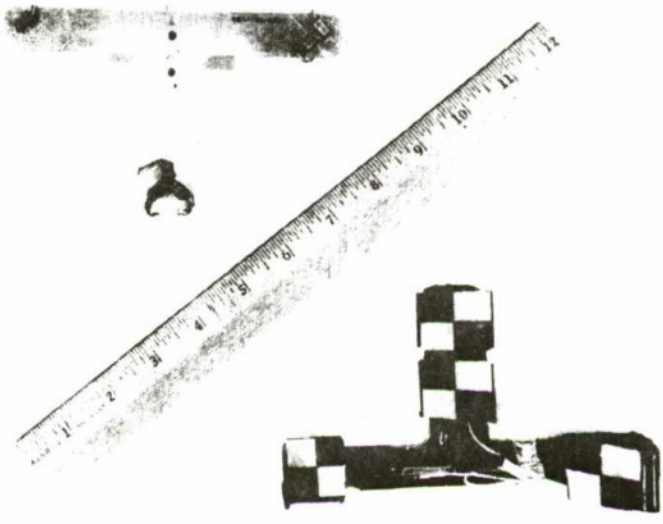

Fig. 3 - Tee-with transducers and the final assembly

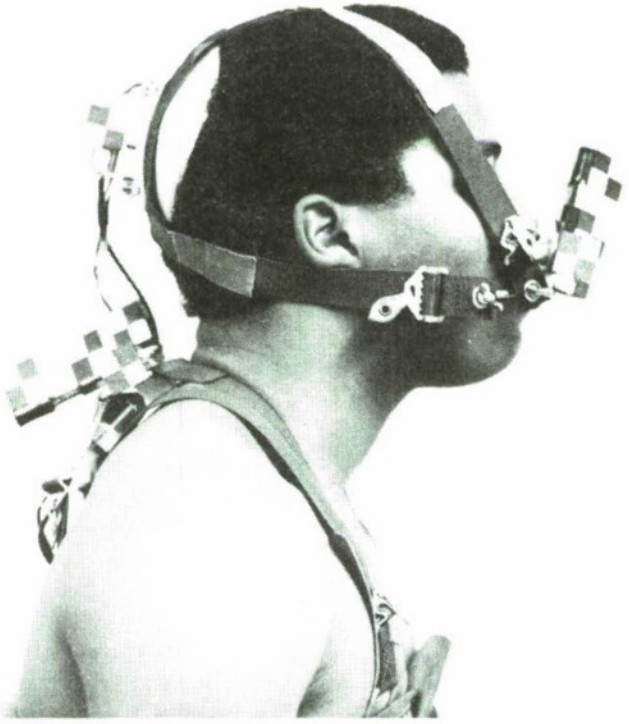

Fig. 4 - Instrumented human volunteer

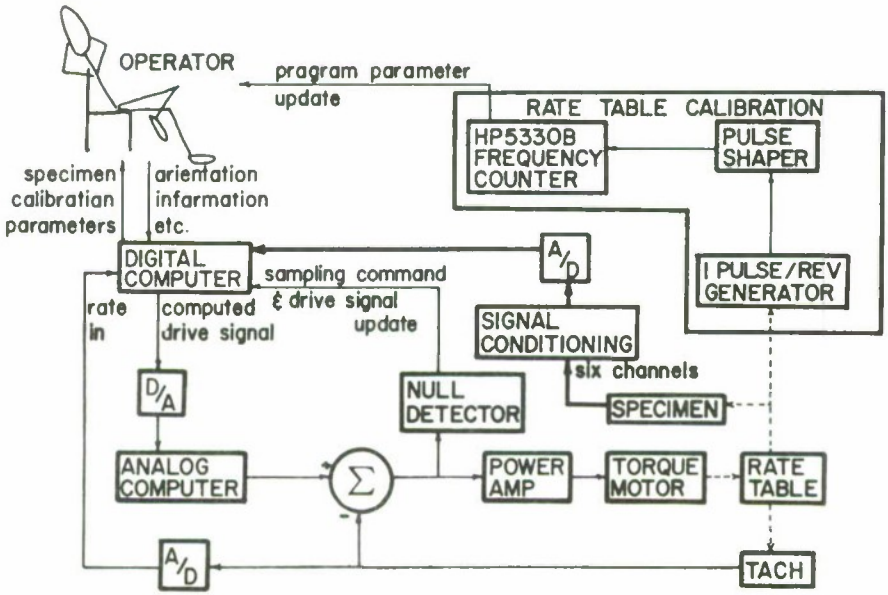

Fig. 5 - The in-house calibration facility

per second; two small turntables mounted on the rate table are used to orient the tracking packages through a wide range of alignments relative to the table's centripetal acceleration.

The calibration procedures call for the package to be mounted on one of the turntables and the requisite orientation information to be entered into the DAS. The DAS then powers up the rate table and takes readings at regularly spaced levels of centripetal acceleration throughout the nominal ranges of the package instrumentation. This operation is repeated for a number of different package orientations.

After six or more such data sets have been collected, the voltage output of each transducer is compared to the inertial accelerations at its inertial mass to obtain a best fit for voltage bias and the components of the sensitive axis. If any of the accelerometers deviate beyond certain limits from this best fit, the package is retired until that unit is replaced. Results based on a number of these calibrations are shown in Figures 6, 7, and 8.

The rate table-computer system is itself periodically calibrated. A device built into the table develops an electrical pulse for each revolution. These pulses are shaped and applied to a Hewlett Packard® 5330 precision time frequency interval counter to assure that the angular velocity of the table is exactly that commanded by the DAS. For acceptable accelerometers, i.e., those meeting certain specified figures of merit, the final output of the calibration procedure consists of the following parameters: sensitivity, offset, direction cosines identifying true sensitive axis direction relative to nominal accelerometer coordinates and rms calibration error. This data is keyed to a tracking package code number and is maintained in a disk file in the DAS to be retrieved each time a package is used in a given experiment.

DATA ACQUISITION

The overall configuration of the DAS used in conjunction with the inertial tracking packages is depicted in Figure 9. The subject borne transducers are connected directly to a set of sled-mounted signal conditioner/line driver amplifiers, the outputs of which are transmitted via the whip cable to the analog console which filters and further amplifies the incoming signals. This console also functions as a central distribution point from which the now buffered and amplified six accelerometer outputs are transmitted not only to the A/D converter for digitization at a rate of 2000 samples per second per channel, but to auxillary recording devices as well.

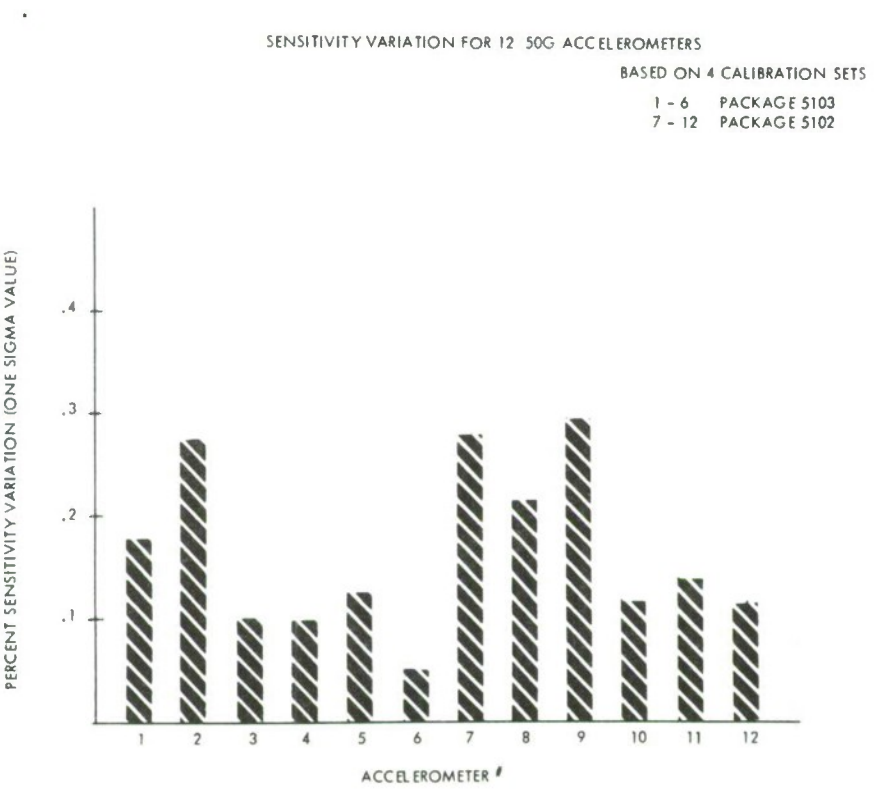

Fig. 6 - Variation in accelerometer sensitivity

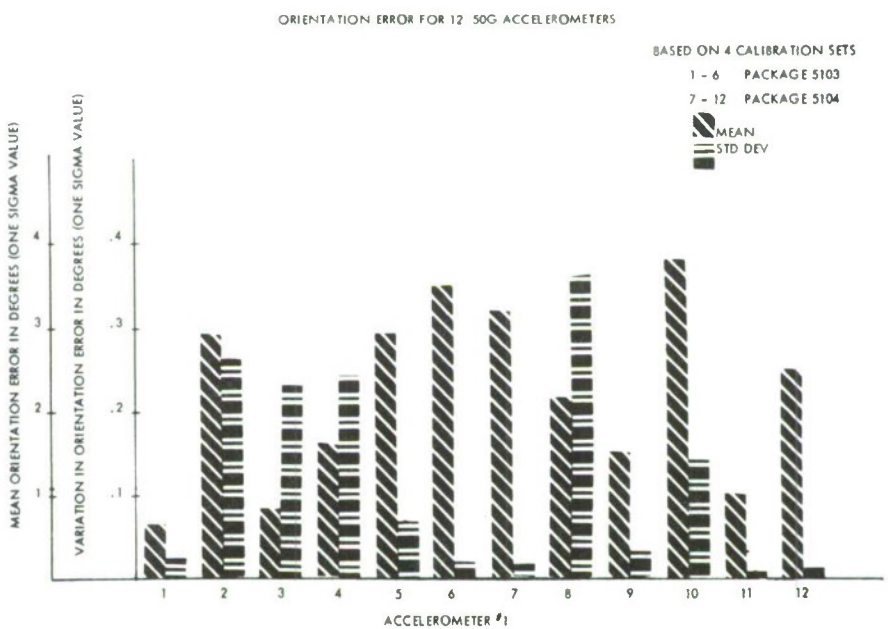

Fig. 7 - Accelerometer alignments – non orthogonality and variation

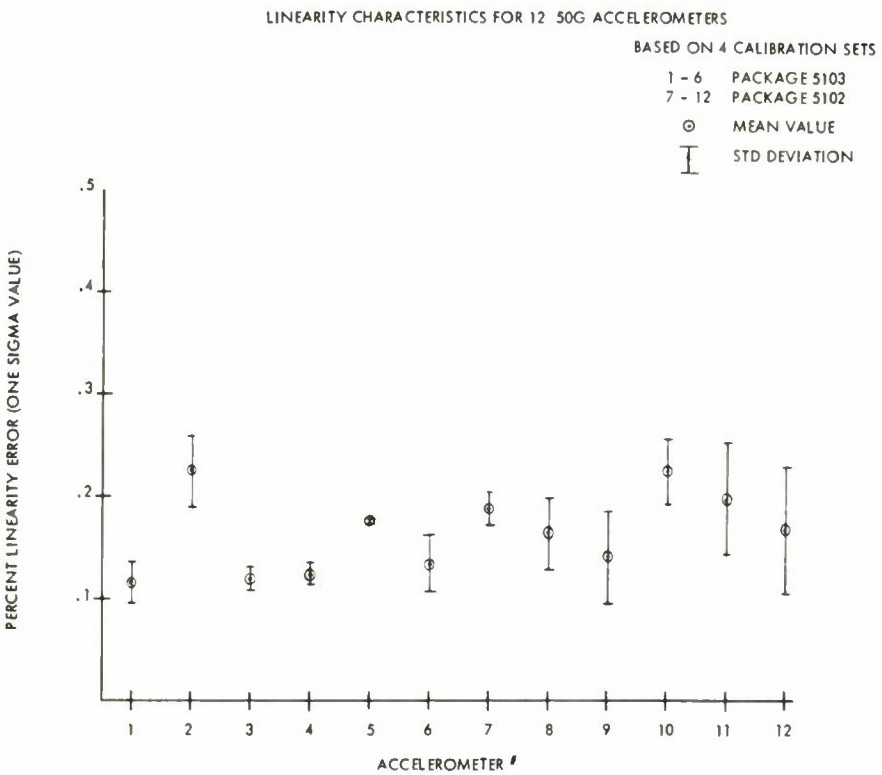

Fig. 8 - Accelerometer linearity

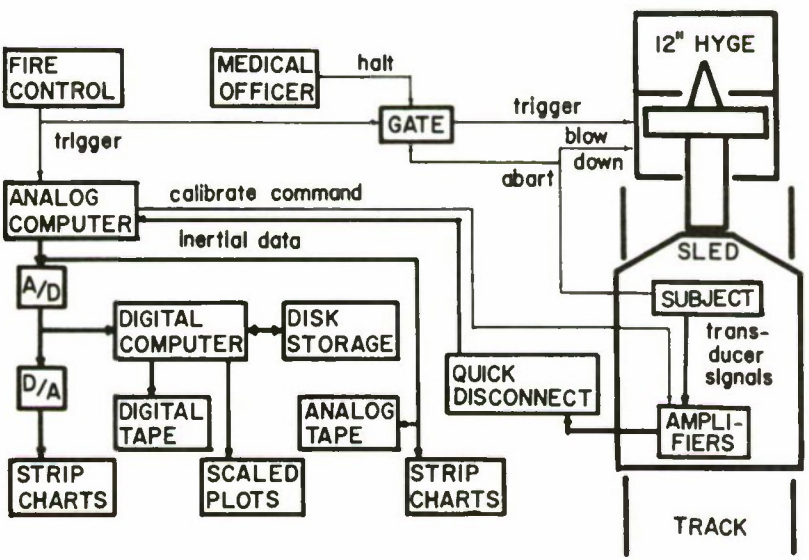

Fig. 9 - The data acquisition system

The gain of a typical data path is continuously adjustable from unity to 500 under computer control. Based upon transducer sensitivity and expected dynamic range of a given experiment, the gain is selected so thot signal-to-noise ratio is maximized.

The calibration of the inertial packages has been previously discussed; the data paths are also exhaustively calibrated immediately prior to eoch experiment. When the sled omplifiers are commanded to the "calibrate" mode, all amplifier inputs are switched from the transducers to a common bus that provides the calibration signal. The calibrotor, on command from the computer, generates a staircase (10-step) signol which is amplified and transmitted by each data path; the calibrator output is also returned to the computer where a comparison is made between it and each path output. Based on this comporison, a total path gain and offset is computed for each channel, based on a least squares fit of the average of 150 samples of each step. An interesting and useful feature of the calibration subsystem is its capability for dynamic optimization of the calibration range. The program, utilizing the transducer sensitivity and signal path gain stored on data files, automatically adjusts the amplitude of the 10-step staircase to span the expected excursions of the transducer outputs during the experiment. Once calibration is completed, the amplifiers are automaticolly reconnected to the transducers.

Inasmuch as each active path is calibrated prior to each run, goin variations about nominol settings are inconsequential, since an exact gain (within measurement error) is computed. The data path parameter of critical importance relotive to overall acquisition accuracy is goin stability, since a gain shift between calibration and acquisition activities (nominally 5-10 minutes) would yield errors. The gain stability achieved by the NAMRL system is depicted in Figure 10, which shows that the variability is inconsequential.

THEORETICAL DEVELOPMENT

The first consideration of the theoretical backgrounds of the inertial tracking packages must be the relationship between the voltage output of an accelerometer and its acceleration environment.

The first assumption is that the voltage output is a function of the translational inertial acceleration of some point in the accelerometer as referenced to the accelerometer axes:

$$Volt = F(A_x, A_y, A_z)$$

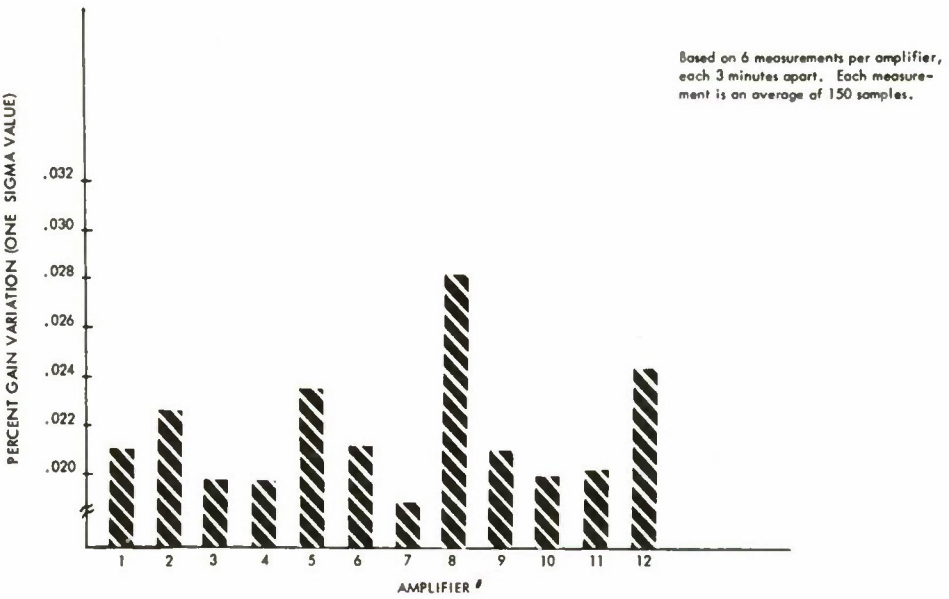

Fig. 10 - Gain stability of the data paths

Taking an expansion around $\underline{A} = 0$ (1)

$$\text{Volt} = \text{Volt}\,|_o + S_x A_x + S_y A_y + S_z A_z$$
$$+ SS_{xx} A_x^2 + SS_{xy} A_x A_y$$
$$+ SS_{xz} A_x A_z + \ldots \quad (2)$$
$$+ SSS_{xxx} A_x^3 + SSS_{xxy} A_x^2 A_y + \ldots$$
$$\vdots$$

If the accelerometer is linear within some region bounded by $|\underline{A}| = \pm A_o$

then

$$\text{Volts} = \text{Volts}\,|_o + S_x A_x + S_y A_y + S_z A_z = \underline{S} \cdot \underline{A} \quad (3)$$

where:

$\text{Volts}|_o$ and S_x, S_y, and S_z are the parameters identified in the calibration procedures.

Body referenced inertial acceleration of a point fixed in o moving rigid body can be expressed as:

$$\underline{A}_p = \underline{A}_o + \dot{\underline{\omega}} \times \underline{P} + \omega \times (\underline{\omega} \times \underline{P}) \tag{4}$$

Where $\underline{A}_o$ is the inertial acceleration of the body referenced frame

$\underline{\omega}$ is angulor velocity of the body

$\dot{\underline{\omega}}$ is the angular acceleration of the body

$\underline{P}$ is the fixed location of the point of interest

The body referenced coordinates are right-handed and orthogonal. Cross products and pseudo vectors are defined according to the right hond rule.

Applying equation (3) to equation (4) the voltage output of an accelerometer whose inertiol mass is locoted at $\underline{P}$ is:

$$\text{Volt} - \text{Volt}|_o = \underline{S} \cdot \underline{A}_o + (\underline{P} \times \underline{S})_{\omega,\omega} - Q \tag{5}$$

Where:

$$\begin{aligned} Q &= \underline{S} \cdot (\underline{\omega} \times (\underline{\omega} \times \underline{P})) \\ &= (\underline{P} \cdot \underline{S})(\underline{\omega})^2 - (\underline{S} \cdot \underline{\omega})(\underline{P} \cdot \underline{\omega}) \end{aligned} \tag{6}$$

Making up six vectors from $\underline{S}$ and $(\underline{P} \times \underline{S})$, and from $\underline{A}_o$ and $\dot{\underline{\omega}}$

$$(\text{Volt} - \text{Volt}|_o) + Q = (\underline{S}, (\underline{P} \times \underline{S})) \cdot (\underline{A}_o, \dot{\underline{\omega}}) \tag{7}$$

Finally, given six such accelerometers, a six vector may be made of quantities corresponding to the left side of equation (7) and a six by six matrix of $(\underline{S}, (\underline{P} \times \underline{S}))$ yielding:

$$(\underline{A}_o, \dot{\underline{\omega}}) = \begin{vmatrix} \vdots & \vdots \\ \underline{S}_n & (\underline{P}_n \times \underline{S}_n) \\ \vdots & \vdots \end{vmatrix}^{-1} \cdot \begin{vmatrix} \vdots \\ (\text{Volt} - \text{Volt}|_o)_n + Q_n \\ \vdots \end{vmatrix} \tag{8}$$

where n represents the n^{th} accelerometer

If the matrix made up of the accelerometer porometers is not ill-conditioned then this procedure will yield the body oriented inertial accelerations.

ERROR ANALYSIS

Assume two sets of inertial accelerations, a physical set and a computational set related as follows to the voltage outputs

$$\text{Volts}_n = (\underline{S}_n , \underline{P}_n \times \underline{S}_n)\cdot(\underline{A}_o , \dot{\underline{\omega}}) - Q_n + \text{Volt}|_{on} \tag{9}$$

and

$$\text{Volts}_n = (\underline{S}_n^1 , \underline{P}_n^1 \times \underline{S}_n^1)\cdot(\underline{A}_o^1 , \dot{\underline{\omega}}^1) - Q_n^1 + \text{Volt}|_{on}^1 + \epsilon_n \tag{10}$$

The primed quantities in equation (10) are the computational counterparts of the physical quantities in equation (9). ϵ_n is a measurement error in determining the accelerometer output.

Equating the right sides of equations (9) and (10) and rearranging

$$\begin{aligned}(A_o^1 , \dot{\omega}^1) = {} & |(S_n^1 , P_n^1 \times S_n^1)|^{-1} \\ & \Big[|(S_n , P_n \times S_n)| \cdot (A_o , \dot{\omega}) \\ & - (Q_n - Q_n^1) + (\text{Volt}|_{on} - \text{Volt}|_{on}^1) \\ & - \epsilon_n \Big]\end{aligned} \tag{11}$$

If $\underline{S}_n^1$ and $\underline{P}_n^1$ correspond to the positions and orientations shown in Figure 1 and differ from their physical counterparts by $\underline{\Delta S}_n$ and $\underline{\Delta P}_n$ then equation (11) becomes

$$\begin{aligned}(A_o^1 , \underline{\dot{\omega}}^1) = {} & (\underline{A}_o , \dot{\underline{\omega}}) + (0,0,0,\omega_2 \omega_3 - \omega_2^1 \omega_3^1 , \\ & \omega_1^1 \omega_3^1 - \omega_1 \omega_3 , \omega_1^1 \omega_2^1 , \omega_1 \omega_2) \\ & + \underline{\underline{M}}_o \cdot (\underline{A}_o , \dot{\underline{\omega}})\end{aligned} \tag{12}$$

$$+ \underline{\underline{M}}_g \cdot (\omega_1^2, \omega_1\omega_2, \omega_2^2, \omega_2\omega_3, \omega_3^2, \omega_3\omega_1)$$

$$+ |(\underline{S}_n^1, \underline{P}_n^1 \times \underline{S}_n^1)|^{-1}$$

$$\cdot (\text{Volt}|_{on} - \text{Volt}|_{on}^1 - \epsilon_n)$$

where $\underline{\underline{M}}_a$ and $\underline{\underline{M}}_g$ are six by six matrices made up of error terms arising out of $\underline{\Delta S}_n$ and $\underline{\Delta P}_n$.

The last four terms on the right side of equation (12) are error terms. The last three of these are similar in scope and magnitude to those that would arise in the nine accelerometer system proposed by King, Padgaonkar, and Krieger (9); by Padgaonkar, Krieger, and King (10); and by Alem (11).

The first of these four error terms is unique to six accelerometer systems. It arises out of the use of computationally determined angular velocities in calculating 'Q_n' which is the centripetal, or gyroscopic, acceleration component being acquired by each accelerometer.

Breoking the equotions for $\dot{\omega}^1$ out of equation (12) gives:

$$\begin{aligned}
\dot{\omega}_1^1 &= \dot{\omega}_1\ \omega_2\ \omega_3 - \omega_2^1\ \omega_3^1 + F_1 \\
\dot{\omega}_2^1 &= \dot{\omega}_2 - \omega_1\ \omega_3 + \omega_1^1\ \omega_3^1 + F_2 \qquad (13) \\
\dot{\omega}_3^1 &= \dot{\omega}_3 - \omega_2\ \omega_1 + \omega_2^1\ \omega_1^1 + F_3
\end{aligned}$$

where F_1, F_2, and F_3 represent the contributions of the last three error terms in equation (12) and are functions of the package trajectory and the accelerometer calibration errors.

Assume very small errors in the computed angular velocities:

$$\underline{\omega}^1 = \underline{\omega} + \underline{e} \qquad (14)$$

Applying equotion (14) to equation (13) and rearranging yields

$$\dot{e}_1 + \omega_3 e_2 + \omega_2 e_3 + e_2 e_3 = F_1$$

$$\dot{e}_2 - \omega_3 e_1 - \omega_1 e_3 - e_2 e_3 = F_2 \qquad (15)$$

$$\dot{e}_3 - \omega_2 e_1 - \omega_1 e_2 - e_1 e_2 = F_3$$

Letting products of the small $\underline{e}$ terms go to zero yields a set of three linear simultaneous differential equations which may now be examined to obtain an understanding of the nature and growth of error in the computed angular velocities.

$$\begin{vmatrix} \dot{e}_1 \\ \dot{e}_2 \\ \dot{e}_3 \end{vmatrix} + \begin{vmatrix} 0 & \omega_3 & \omega_2 \\ -\omega_3 & 0 & -\omega_1 \\ -\omega_2 & -\omega_1 & 0 \end{vmatrix} \cdot \begin{vmatrix} e_1 \\ e_2 \\ e_3 \end{vmatrix} = \begin{vmatrix} F_1 \\ F_2 \\ F_3 \end{vmatrix} \qquad (16)$$

Letting

$$\underline{\omega} = \underline{n}\,\Omega_o \qquad (17)$$

$$\phi_o = \int_{\Omega_o}^{t} dt$$

Where $\underline{n}$ is a unit vector, Ω_o the magnitude of ω is a scalar function of time and ϕ_o is a time integral of Ω_o and will be called, for convenience, angular displacement.

Applying (17) to (16), dividing through by Ω_o, and invoking the chain rule yields

$$\begin{vmatrix} \overset{*}{e}_1 \\ \overset{*}{e}_2 \\ \overset{*}{e}_3 \end{vmatrix} + \begin{vmatrix} 0 & n_3 & n_2 \\ -n_3 & 0 & -n_1 \\ -n_2 & -n_1 & 0 \end{vmatrix} \cdot \begin{vmatrix} e_1 \\ e_2 \\ e_3 \end{vmatrix} = \begin{vmatrix} F_1/\Omega_o \\ F_2/\Omega_o \\ F_3/\Omega_o \end{vmatrix} \qquad (18)$$

Where * indicates differentiation with respect to ϕ_o which must be a monotomically increasing function of time.

The related set of homogeneous equations is:

$$\underline{e}^{1} + \begin{vmatrix} 0 & n_3 & n_2 \\ -n_3 & 0 & -n_1 \\ -n_2 & -n_1 & 0 \end{vmatrix} \underline{e} = 0 \qquad (19)$$

For n_1 near zero the eigenvalues are

$$\lambda_1 \simeq 2 \; n_1 \; n_2 \; n_3$$

$$\lambda_2 \simeq \sqrt{-1} - n_1 \; n_2 \; n_3 \qquad (20)$$

$$\lambda_3 \simeq - \sqrt{-1} - n_1 \; n_2 \; n_3$$

Suggesting that $\underline{e}$ is a nearly sinusoidal function of angular displacement. In the region where n_1 approaches 1 however;

$$\lambda_1 = 0$$

$$\lambda_2 = 1 \qquad (21)$$

$$\lambda_3 = -1$$

By putting the eigenvalue equation in polar coordinates such that n_1 corresponds to the polar axis it can be shown that λ_3 is at a local minimum and λ_2 at a local maximum.

Even so, $\underline{e}$ has components that vary as an exponential function of the angular displacement, but since this quantity is never much greater than a quarter of a revolution and is, in fact, generally much less for biodynamic impact acceleration, study of these homogeneous equations shows a worst case error of less than a five-fold increase of the initial error in angular velocity. Since the initial value of angular velocity can be so closely controlled this increase is negligible.

The nonhomogeneous components of the solution to equation (18) for axes normal to the X axis are, as might be expected, mostly well behaved sinusoids along with the types of error that generally occur in straightforward integration. The worst case is again, rotation about the X axis.

Invoking techniques from Kaplan (12), the nonhomogeneous components for this case are:

$$\int^t F_1 \, dt \qquad (22)$$

and:

$$\text{Exp}(\phi)\int^{t}((F_2 + F_3)\,\text{Exp}(-\phi))\,dt \pm \text{Exp}(-\phi)\int^{t}((F_2 - F_3)\,\text{Exp}(\phi)\,dt \tag{23}$$

where expression (22) represents the on-axis solution and (23) represents the two aff-axis solutions. For angular displacements on the order of a quarter of a revolution expression (23) serves to treble or quadruple the errors that could be expected if it were not necessary to calculate Q_n using integrations of the computed angular accelerations. But if these sources of error in $\underline{F}$ are minimized, as has been done by: Preselection of the inertial transducers; periodic on-site calibration of the packages; routine calibration of the datapaths prior to each experiment; and on line digitization of the analog signals, then even the worst case errors in expression (23) become acceptable.

EXPERIMENTAL SET UP

The $-G_x$ impact experiments currently in progress at this laboratory have been described in a number of reports. (1), (13) The essence of these descriptions is that human volunteers equipped with anatomically mounted inertial tracking packages located at the mouth and the posterior spinaus pracess af the first thoracic vertebral bady are exposed ta short duratian accelerations approximating a frontal (eye balls aut) crash impact.

The position and orientation of the tracking packages relative to coordinate systems located in the bony anatomy of their mounting sites is measured using radiographic techniques developed at this laboratory. This information is then applied to the mathematical procedures already described so that the final output of the camputations is the time history of the motion af the anatomical coordinate system relative to a coordinate system fixed in the laboratory.

RESULTS

The results of a number of these impact experiments have been prepared to demonstrate the workability of the inertial tracking packages. Since many of the experiments include subject mounted

rate gyroscopes as redundant instrumentation, a check is available on the calculated angular velocity about the subject Y axis.

This axis runs approximately right to left in the body according to the definitions in reference (4) so that the motion for the head produced by such an angular velocity would be a nodding motion. The rotation produced by $-G_x$ impact takes place primarily about this axis.

Figure 11 compares time histories of head angular velocities about this Y axis as obtained from the rate gyroscopes (*) and the inertial tracking packages (•). Since the rate gyroscopes behave as a second order low-pass filter with a natural frequency of 37 Hz, and a damping ratio of .5, a similar plot was prepared, figure 12, in which the output from the inertial tracking package was altered to approximate the effect of this filtering.

Off-axis components of the rotational motion are addressed by a second technique. The sensitivities of certain transducers were incremented or decremented by .5% prior to calculation of the trajectories in order to generate a worst case error envelope about the solution for a 10 g, $-G_x$ impact.

Figures 13 through 21 show the three body-oriented angular velocities, the lab oriented three translational accelerations, and the three body oriented angular accelerations as measured and calculated for the head. Figures 22 through 30 show the same information for T-1, the first thoracic vertebral body.

The divergence of the envelope (+) and (*) from the solution (•) for the head angular velocities at 250 milliseconds is about 5% of the peak magnitude of the head angular velocity. This divergence is much greater than that shown for the motion of T-1, and, since the head moves through an angle of 82° versus 15° for T-1, this observation bears out the conclusions concerning the effect of angular displacement brought out in the theoretical development.

CONCLUSIONS

A set of six accelerometers is sufficient to measure rigid body motion for certain types of trajectories. The requirements for these trajectories are that angular displacement not be much greater than a quarter of a revolution and that the accelerations themselves have no sharp peaks as might be produced by striking other rigid objects.

The first of these requirements is necessitated by the feedback caused by gyroscopic acceleration terms, and the second by the

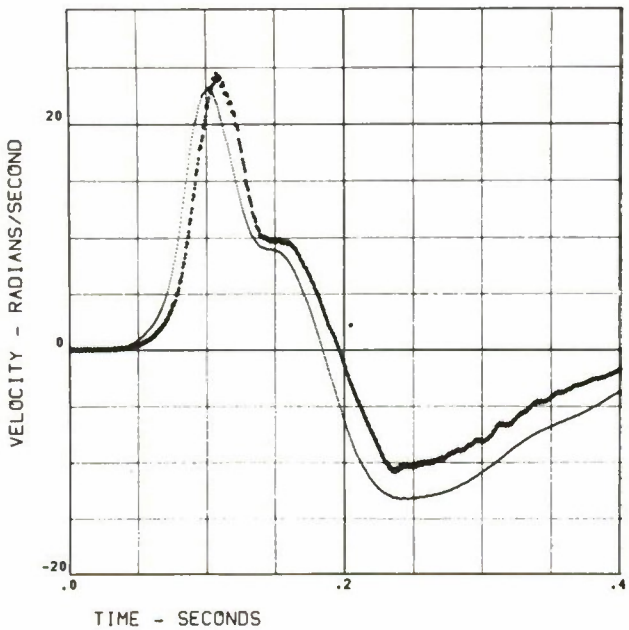

Fig. 11 - Comparison of angular velocity measured by rate gyroscope (*) and that derived from an inertial tracking package ( )

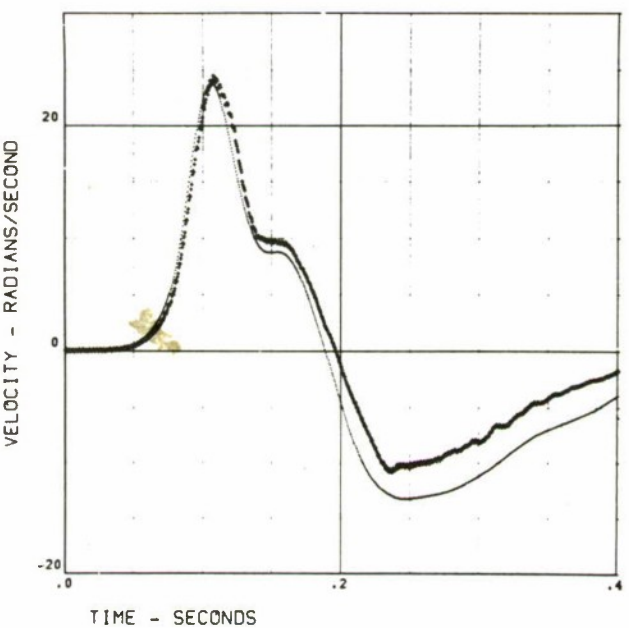

Fig. 12 - Comparison of angular velocity measured by rate gyroscope (*) and that derived from an inertial tracking package ( ) in which variations in bandpass are eliminated

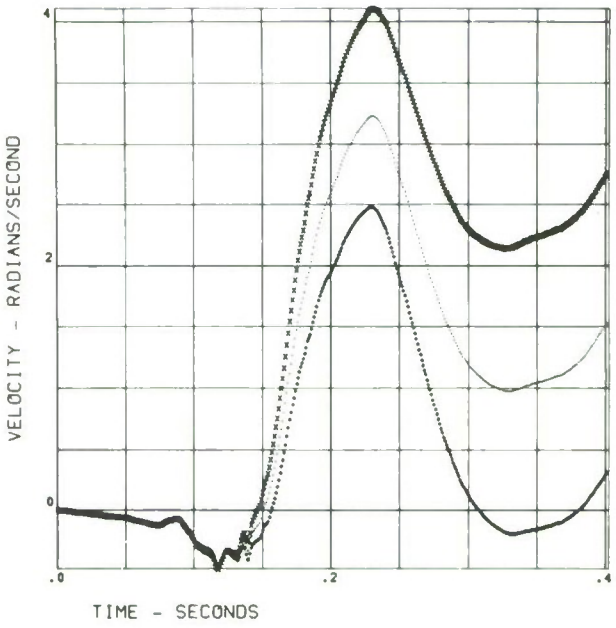

Fig. 13 - Head X angular velocity ( ) and envelope (*), (+)

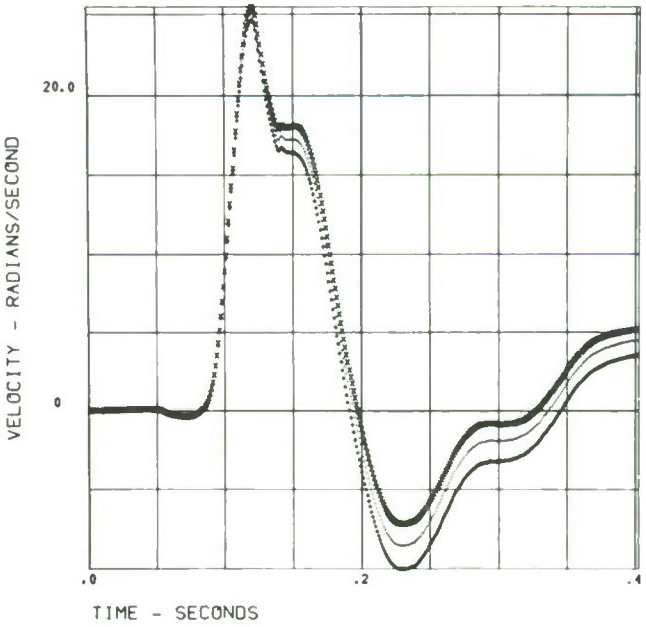

Fig. 14 - Head Y angular velocity

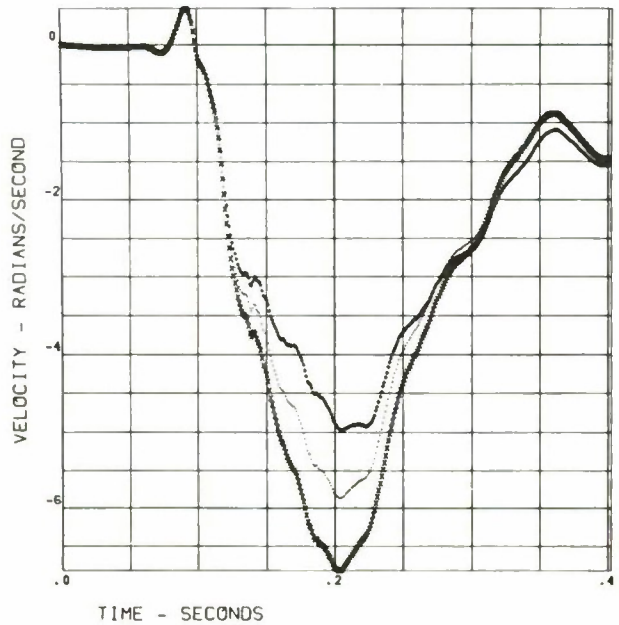

Fig. 15 - Head Z angular velocity

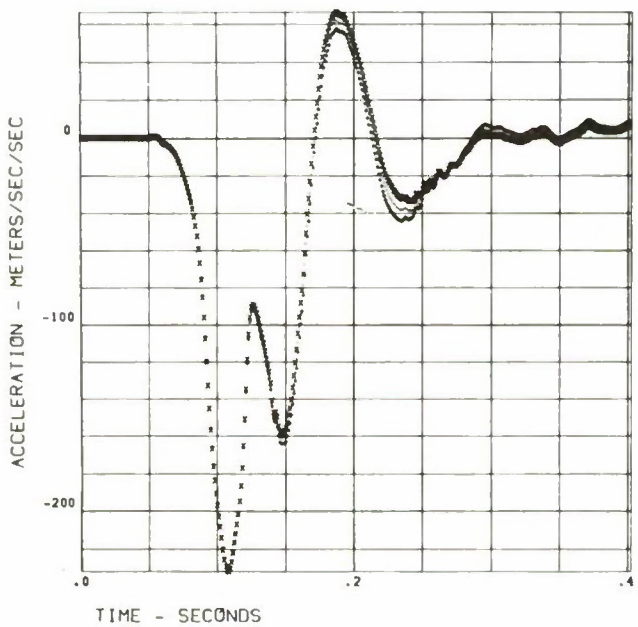

Fig. 16 - Head X translational acceleration

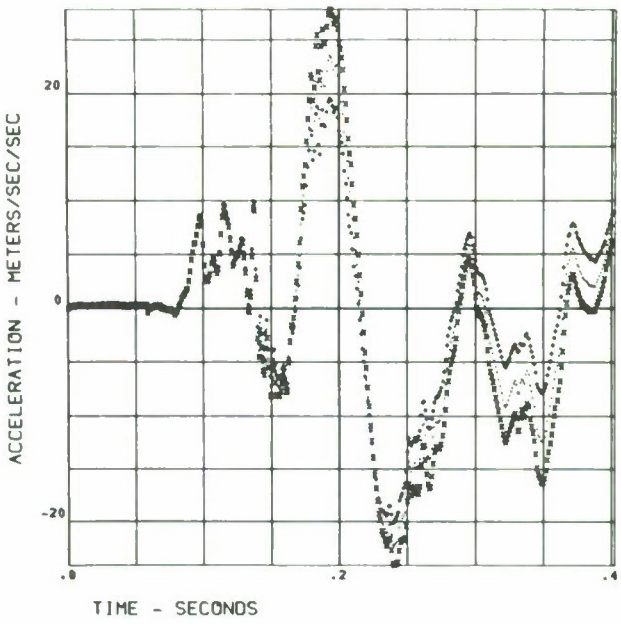

Fig. 17 - Head Y translational acceleration

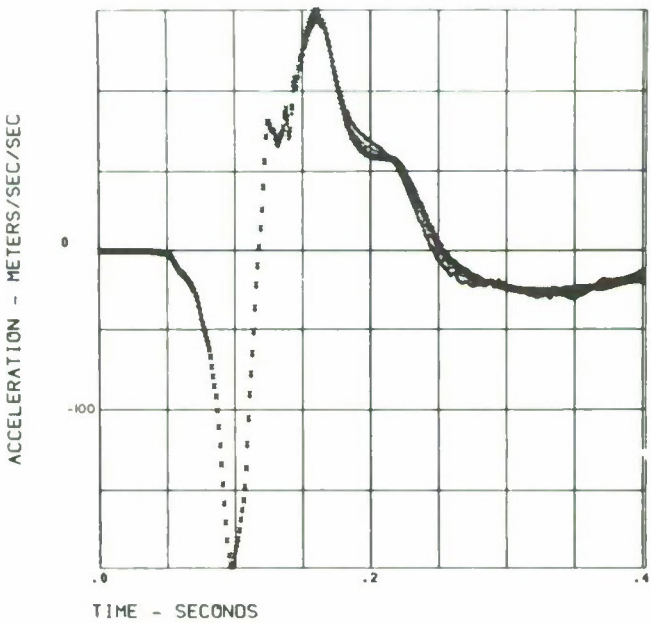

Fig. 18 - Head Z translational acceleration

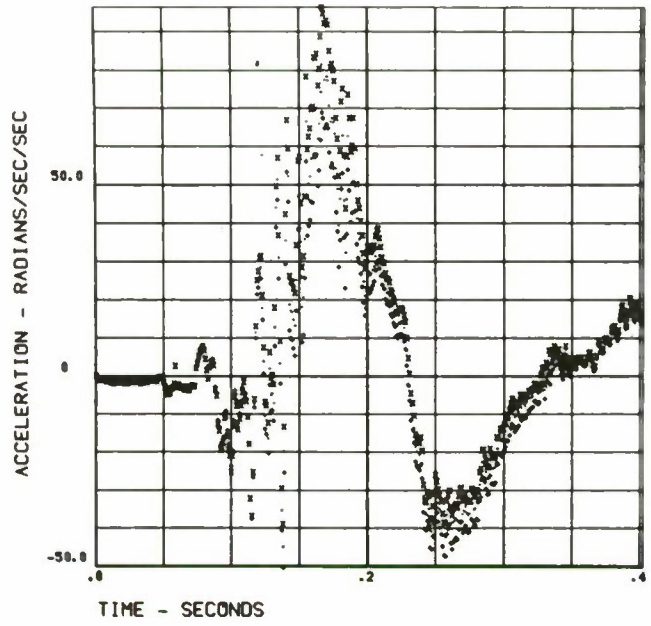

Fig. 19 - Head X angular acceleration

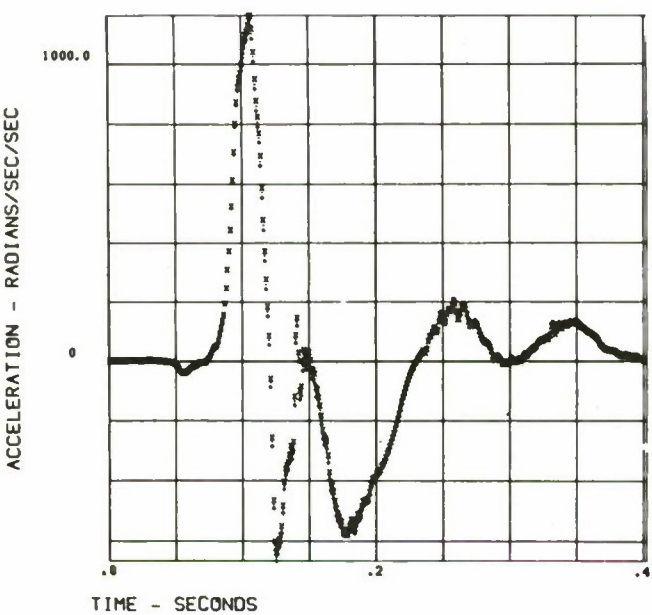

Fig. 20 - Head Y angular acceleration

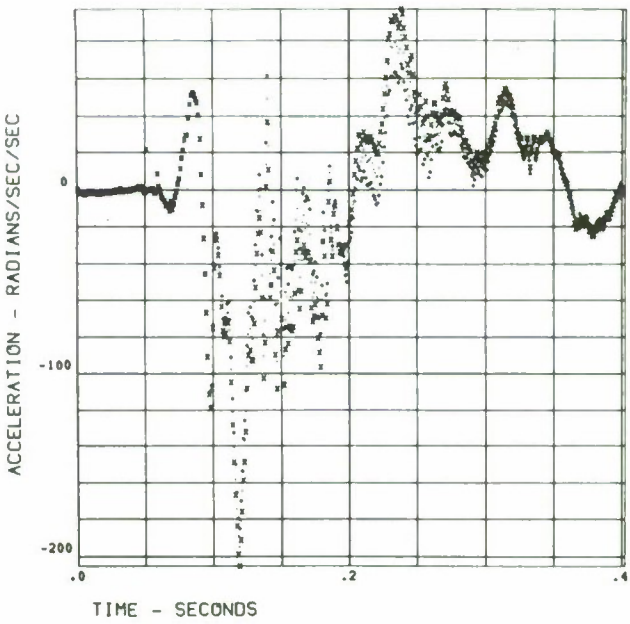

Fig. 21 - Head Z angular acceleration

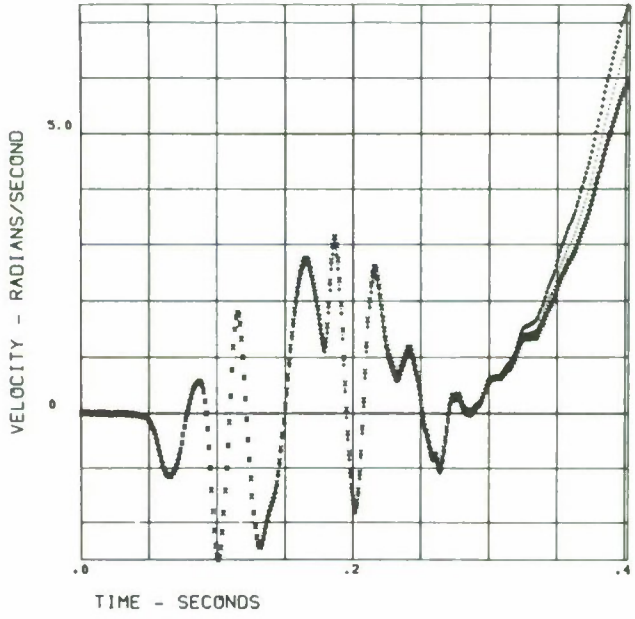

Fig. 22 - First thoracic vertebral body (T-1) X angular velocity

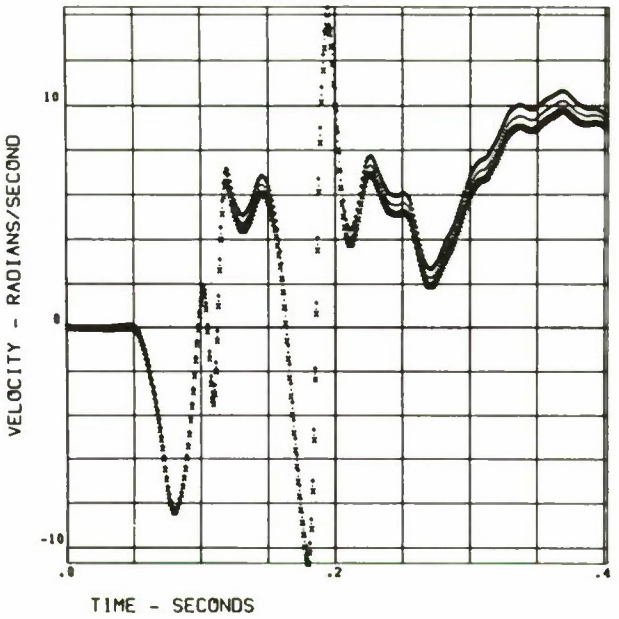

Fig. 23 - T-1 Y angular velocity

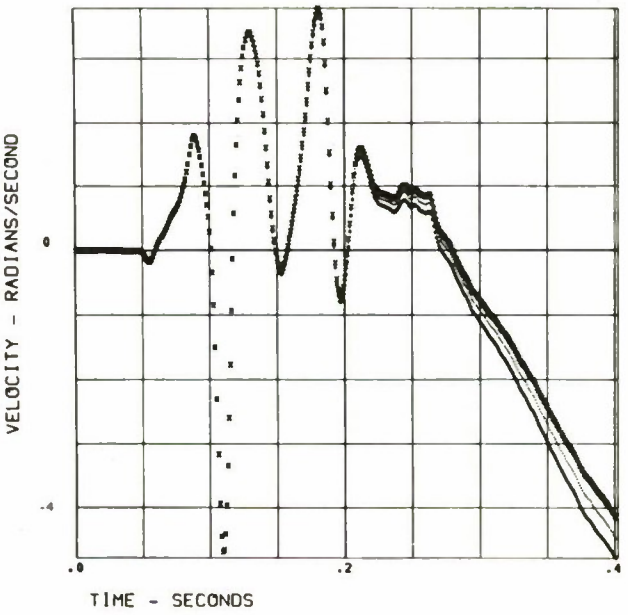

Fig. 24 - T-1 Z angular velocity

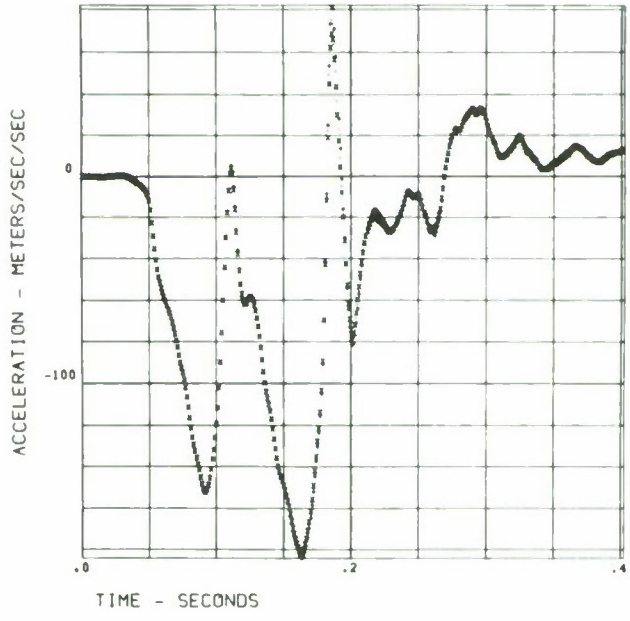

Fig. 25 - T-1 X translational acceleration

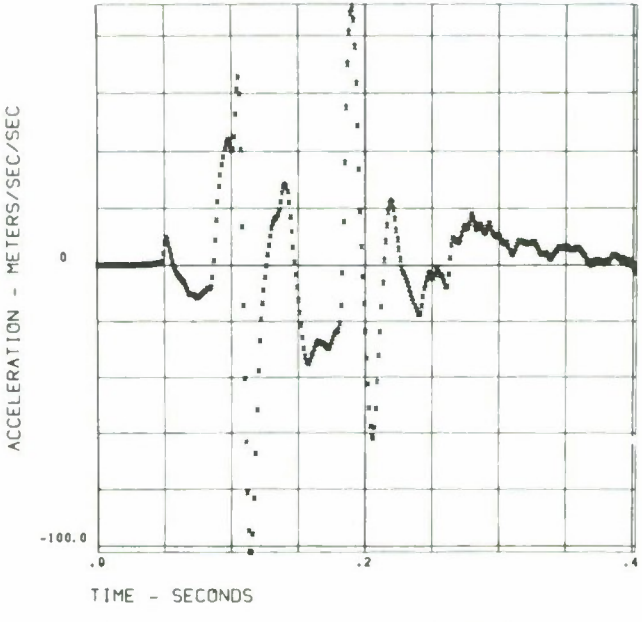

Fig. 26 - T-1 Y translational acceleration

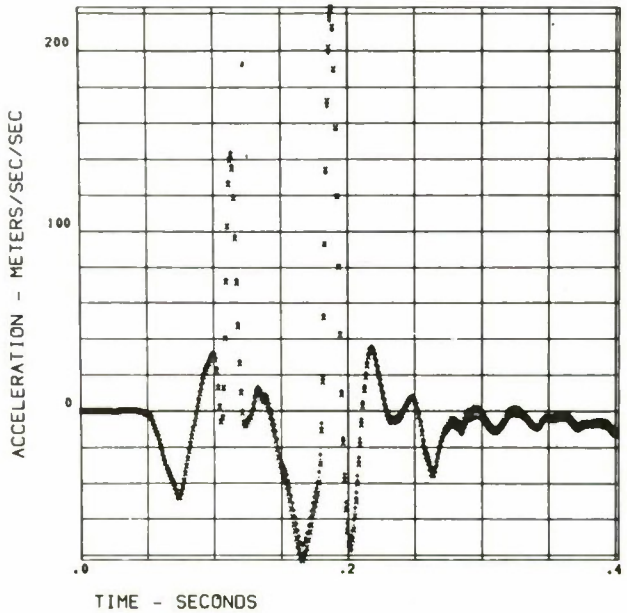

Fig. 27 - T-1 Z translational acceleration

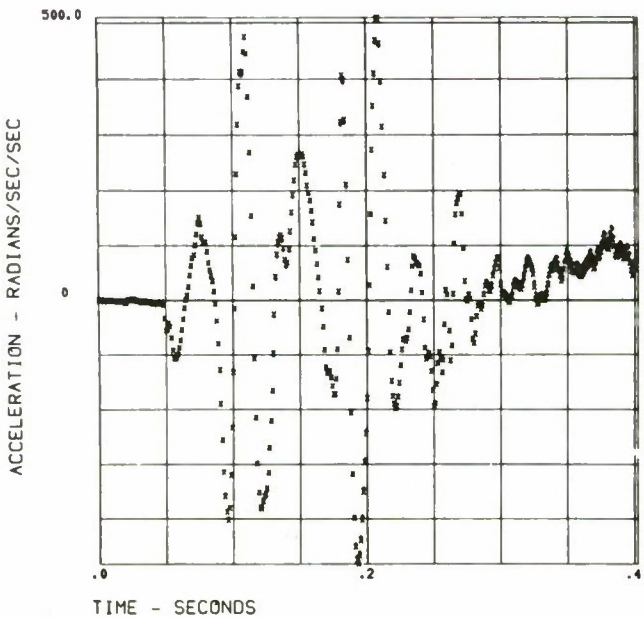

Fig. 28 - T-1 X angular acceleration

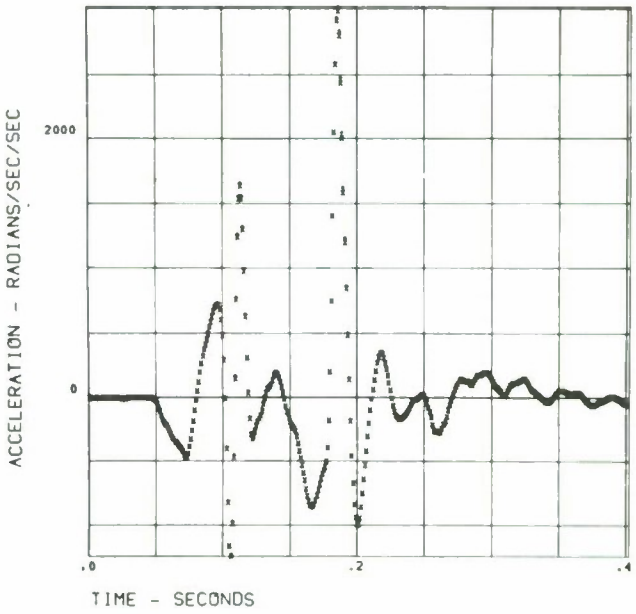

Fig. 29 - T-1 Y angular acceleration

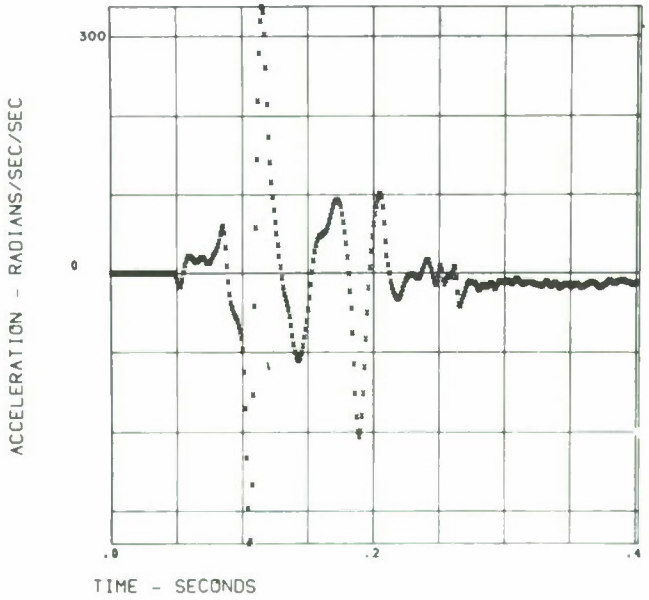

Fig. 30 - T-1 Z angular acceleration

need for favorable scaling in minimizing the error terms in the calculation. This minimization of error terms is itself made much more critical by the gyroscopic acceleration terms imposing the need for on-site calibration facilities as well as calibrating sensitivities as vectors rather than idealizing them in terms of orthogonal alignments.

Human dynamic response to impact acceleration for cases where no direct contact with obstructions is permitted results in trajectories falling within the herein specified limits. If the problems of anatomically mounting such sets of six accelerometers can be overcome, i.e. those of relative motion, added mass, restrictive strapping, etc., then the output of these transducers will yield the kinematic parameters of the body motion.

REFERENCES

1. E. B. Becker, "A Photographic Data System for Determination of 3 Dimensional Effects of Multiaxes Impact Acceleration on Living Humans." Submitted for publication, Automotive Safety Seminar SPIE, December 1974.

2. C. L. Ewing, D. J. Thomas, G. W. Beeler, L. M. Patrick, and D. B. Gillis, "Dynamic Response of the Head and Neck of the Living Human to $-G_x$ Impact Acceleration." Proceedings of the Twelfth Stapp Car Crash Conference, New York, Society of Automotive Engineers, Inc., 1968.

3. C. L. Ewing, D. J. Thomas, L. M. Patrick, G. W. Beeler, and M. J. Smith, "Living Human Dynamic Response to $-G_x$ Impact Acceleration II - Accelerations Measured on the Head and Neck." Proceedings of the Thirteenth Stapp Car Crash Conference, New York, Society of Automotive Engineers, Inc., 1969.

4. C. L. Ewing and D. J. Thomas, "Human Head and Neck Response to Impact Acceleration." NAMRL Monograph 21, Pensacola Naval Air Station, Pensacola, Florida, 1972.

5. C. D. Bendixen, "Measurement of Head Angular Acceleration During Impact." ARL-TR-70-5, Hollaman Air Force Base, New Mexico, 1970.

6. T. D. Clarke, C. D. Gragg, J. F. Sprouffser, E. M. Trout, R. M. Zimmerman, and W. H. Muzzy, "Human Head Linear and Angular Accelerations During Impact." Proceedings of the Fifteenth Stapp Car Crash Conference, New York, Society of Automotive Engineers, Inc., 1971.

7. H. J. Mertz and L. M. Patrick, "Strength and Response of the Human Neck." Proceedings of the Fifteenth

Stapp Car Crash Conference, New York, Society of Automotive Engineers, Inc., 1971.

8. E. B. Becker, "Measurement of the Mass Distribution Parameters of Anatomical Segments." Proceedings of the 16th Stapp Car Crash Conference, New York, Society of Automotive Engineers, Inc., 1972.

9. A. I. King, A. J. Padgaonkar, and K. W. Kreiger, "Measurement of Angular Acceleration of A Rigid Body Using Linear Accelerometers." Proceedings of the 2nd Annual International Meeting of the Ad Hoc Committee on Human Subjects for Biomechanical Research, Ed., A. E. Hirsch.

10. A. J. Padgaonkar, K. W. Kreiger, A. I. King, "Measurement of Angular Acceleration of a Rigid Body Using Linear Accelerometers." Paper No. 75-APMB-3, Presented at the ASME Applied Mechanics Summer Conference Symposium on Biomechanics, Rensselaer Polytechnic Institute, Troy, New York, June 1975.

11. N. M. Alem, "The Measurement of 3-D Rigid Body Motion." Proceedings of the 2nd Annual International Meeting of the Ad Hoc Committee on Human Subjects for Biomechanical Research, Ed., A. E. Hirsch.

12. W. Kaplan, "Ordinary Differential Equations." Addison-Wesly Publishing Co., Inc., 1958.

13. C. L. Ewing, D. J. Thomas, L. Lustick, E. Becker, G. Willems, and W. Muzzy, "The Effect of Initial Position of the Head and Neck on the Dynamic Response of the Human Head and Neck to -G$_x$ Impact Acceleration." Submitted for presentation at the 19th Stapp Car Crash Conference, San Diego, California, November 1975.

ACKNOWLEDGEMENTS

The work was funded by the Naval Medical Research and Development Command and by the Biological Sciences Division of the Office of Naval Research. Opinions or conclusions contained in this report do not necessarily reflect the views or endorsement of the Navy Department.

Trade names of materials or products of commercial or non-Government organizations are cited only where essential to precision in describing research procedures or evaluation of results. Their use does not constitute official endorsement or approval.

To Gloria Bourgeois, who assisted in the preparation of this report; Channing L. Ewing, Daniel J. Thomas, Gerald Williamson,

Leonard S. Lustick, William Anderson, and William Muzzy; to William Caplan of Entran Devices, Inc., and mast importantly ta the valunteer subjects; the authars extend their most grateful appreciatian.